Letter

Photonic heat transport through a Josephson junction in a resistive environment

A. Levy Yeyati [1,2,3] D. Subero,[4] J. P. Pekola [4] and R. Sánchez [1,2,3]

[1]*Departamento de Física Teórica de la Materia Condensada, Universidad Autónoma de Madrid, 28049 Madrid, Spain*
[2]*Condensed Matter Physics Center (IFIMAC), Universidad Autónoma de Madrid, 28049 Madrid, Spain*
[3]*Instituto Nicolás Cabrera, Universidad Autónoma de Madrid, 28049 Madrid, Spain*
[4]*PICO Group, QTF Centre of Excellence, Department of Applied Physics, Aalto University School of Science, P.O. Box 13500, 0076 Aalto, Finland*

(Received 21 March 2024; revised 17 June 2024; accepted 25 November 2024; published 6 December 2024)

Motivated by recent experiments [Subero *et al.*, Nat. Commun. **14**, 7924 (2023)], we analyze photonic heat transport through a Josephson junction in a dissipative environment. For this purpose, we derive general expressions for the heat current in terms of nonequilibrium Green's functions for the junction coupled in series or in parallel with two environmental impedances at different temperatures. We show that even on the insulating side of the Schmid transition, the heat current is sensitive to the Josephson coupling exhibiting an opposite behavior for the series and parallel connection and in qualitative agreement with experiments. We also predict that this device should exhibit heat rectification properties and provide simple expressions to account for them in terms of the system parameters.

DOI: 10.1103/PhysRevB.110.L220502

Introduction. The physics of Josephson junctions (JJs) has attracted great interest for many decades [1]. Even the apparently simple case of a single JJ in a resistive environment provides a rich playground to study the interplay of quantum tunneling and dissipation [2], which continues to be explored to this today [3,4]. For this system, a transition between a superconducting and an insulating phase was predicted to appear as a function of the environmental resistance (R), regardless of the Josephson coupling energy (E_J). This is the so-called Schmid-Bulgadaev (SB) transition [5,6], which has been the object of intense theoretical [7–11] and experimental debate in recent years [12–14].

In spite of this intense activity, little is known regarding this system's properties beyond dc charge transport. In this respect, heat transport [15] can provide additional insights. In a recent experiment, Subero *et al.* [16] explored heat transport through a JJ in the supposedly insulating regime ($R > R_Q = h/4e^2$). Even when charge transport could be well described by dynamical Coulomb blockade theory, it was found that heat transport was sensitive to the E_J value (tunable through a magnetic flux in a SQUID configuration), indicating inductive response at high frequencies. The experimental results were fitted using a phenomenological theory, including an inductive term to the junction effective impedance. However, such a model is incompatible with the mentioned dc charge transport properties and apparently in conflict with a SB transition.

In the present Letter, we analyze this problem from a microscopic perspective. For this purpose, we develop a nonequilibrium Green's function (GF) approach which takes into account interaction effects due to finite E_J/E_c values, where E_c is the junction charging energy. We find that even for $R > R_Q$, heat transport is sensitive to the Josephson coupling, in qualitative agreement with experiments. Moreover, we find that the heat current response is radically different depending on whether the junction is connected in parallel or in series to the source and drain leads. We also show that signatures of the SB transition in the heat conduction appear at sufficiently low temperatures. We finally demonstrate that asymmetric devices exhibit heat rectification properties, which provide an alternative way to detect the SB transition.

In Fig. 1, we schematically represent the two situations to be considered: In Fig. 1(a), the JJ is connected in parallel with the left and right resistors (R_L and R_R) which are held at temperatures T_L and T_R, respectively, whereas in Fig. 1(b) these circuit elements are connected in series, corresponding to the experimental configuration in Ref. [16]. The aim of the theory is to determine the resulting heat current J as a function of the model parameters in these two situations, assuming that temperatures are low enough to neglect excited quasiparticles in the superconducting leads.

Parallel configuration. Let us start with the parallel configuration [17]. This is modeled by the following Hamiltonian:

$$H = E_c N^2 - E_J \cos\varphi - \sum_{j,k}\left[\lambda_{j,k}(a_{jk} + a_{jk}^\dagger)\varphi - \frac{\lambda_{jk}^2}{\hbar\omega_{jk}}\varphi^2\right] + \sum_{j,k}\omega_{jk}a_{jk}^\dagger a_{jk}, \tag{1}$$

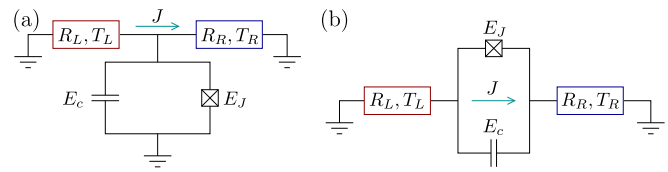

FIG. 1. Schematics of the configurations considered, consisting of two resistors, R_L and R_R, connected in (a) parallel and (b) series to a Josephson junction (defined by a Josephson, E_J, and a charging energy E_c), and holding different temperatures, T_L and T_R, that lead to a heat current J.

where $j \equiv L, R$ and the dissipative terms satisfy

$$\frac{\pi}{2}\sum_k \lambda_{jk}^2 \delta(\omega-\omega_{jk}) = \frac{\hbar^2\omega}{4e^2}\mathrm{Re}\left[\frac{1}{Z_j(\omega)}\right],$$

$Z_j(\omega)$ being the lead impedances, which in our case correspond to pure resistances R_j. In this configuration. only one superconducting phase variable, φ, conjugate to the charge which is transferred through the junction, N, plays a role.

Following Ref. [18], the heat current through lead j can then be computed as

$$\begin{aligned} J_j &= \langle \dot{H}_j\rangle = -i\sum_k \lambda_{jk}\omega_{jk}[\langle a_{jk}(t)\varphi(t)\rangle - \text{H.c.}] \\ &= 2\sum_k \lambda_{jk}\omega_{jk}\mathrm{Re}G^{+-}_{a_{jk},\varphi}(t,t)\,, \end{aligned} \tag{2}$$

where $G^{\alpha\beta}_{A,B}(t,t') = -i\langle T_C B(t')A(t)\rangle$ denotes the Keldysh $\alpha\beta$ GF associated with operators A, B. Using the equation of motion method and transforming it into frequency representation, one can express $G^{+-}_{a_{jk},\varphi}$ as

$$G^{+-}_{a_{jk},\varphi}(\omega) = \lambda_{jk}\big[D^r(\omega)g^{+-}_{a_{jk}}(\omega) + D^{+-}(\omega)g^a_{a_{jk}}(\omega)\big], \tag{3}$$

where the $g^{+-,a}_{a_{jk}}$ correspond to the uncoupled leads and, for simplicity, we denote $D^{\alpha\beta,r,a} \equiv G^{\alpha\beta,r,a}_{\varphi\varphi}$ (the superscripts r, a indicate the retarded, advanced components). In this way, we can express the heat current as

$$J_j = 2\sum_k \lambda_{jk}^2\omega_{jk}\int\frac{d\omega}{2\pi}\mathrm{Re}\big[D^r(\omega)g^{+-}_{a_{jk}}(\omega) + D^{+-}(\omega)g^a_{a_{jk}}(\omega)\big]. \tag{4}$$

We can further use $g^{+-}_{a_{jk}}(\omega) = -2\pi i n_j(\omega_{jk})\delta(\omega-\omega_{jk})$ and $g^a_{a_{jk}}(\omega) = 1/(\omega-\omega_{jk}-i0^+)$, where $n_j(\omega)$ denotes the Bose function for the modes in the j lead. Replacing these in Eq. (4) and taking the real part, we obtain

$$\begin{aligned} J_j = \int\frac{d\omega}{2\pi}\frac{\hbar^2\omega^2}{e^2}&\mathrm{Im}\left[D^r(\omega)\coth\left(\frac{\omega\beta_j}{2}\right) - \frac{D^K(\omega)}{2}\right] \\ &\times\ \mathrm{Re}\left[\frac{1}{Z_j(\omega)}\right], \end{aligned} \tag{5}$$

where we have introduced the Keldysh GFs $D^K = D^{+-} + D^{-+}$ in the triangular representation [19] and $\beta_j = 1/k_B T_j$. Further simplification is obtained if, as in our case, the lead admittances $1/Z_j(\omega) \equiv 1/R_j$ are frequency independent. Then, imposing heat current conservation $J_R = -J_L = J$, one gets [18]

$$J = -\frac{\hbar^2}{2\pi e^2}\int d\omega\frac{\omega^2\mathrm{Im}D^r(\omega)}{R_L+R_R}[n_L(\omega)-n_R(\omega)]\,, \tag{6}$$

which is the heat transport analog of the Meir-Wingreen formula for mesoscopic charge transport [20], allowing us to define an effective heat transmission coefficient for the parallel configuration

$$\tau^{\text{eff}}_{\text{parallel}}(\omega) = -\frac{4\eta_L\eta_R\omega\mathrm{Im}D^r(\omega)}{\eta_L+\eta_R}\,, \tag{7}$$

where $\eta_j = R_Q/(2\pi R_j) \equiv \alpha_j/2\pi$. One can further check that for the perfect-transmission case, one gets $J = J_{\max} \equiv \pi k_B^2(T_L^2 - T_R^2)/(12\hbar)$ as it corresponds to a ballistic channel [21].

Perturbation theory. The problem is thus mapped into the evaluation of the Keldysh GFs $D^{r,a,K}(\omega)$. In the present Letter, we focus on the regime $R_{L,R} \gtrsim R_Q$ and $E_J < E_c$ for which perturbation theory in E_J should be valid and which should be appropriate to describe the experimental results of Ref. [16]. To zeroth order in E_J, the GFs are given by

$$\begin{aligned} D_0^{r,a}(\omega) &= \frac{1}{m\omega^2 \pm i\omega(\eta_L+\eta_R) - m\omega_c^2}, \\ D_0^K(\omega) &= \frac{-2i\omega(\eta_L(1+2n_L(\omega)) + \eta_R(1+2n_R(\omega))}{\left(m\left(\omega^2-\omega_c^2\right)\right)^2 + (\omega(\eta_L+\eta_R))^2}\,, \end{aligned} \tag{8}$$

where $m = \hbar/2E_c$ and ω_c is a small frequency cutoff which warrants convergence in the Fourier transforms. At zeroth order in E_J and $\omega_c \to 0$, from (7) we obtain

$$\tau^0_{\text{parallel}}(\omega) = \frac{4\eta_L\eta_R}{(m\omega)^2 + (\eta_L+\eta_R)^2}\,, \tag{9}$$

which reaches a maximum value $4\eta_L\eta_R/(\eta_L+\eta_R)^2$ at zero frequency.

Higher order corrections can be introduced through the self-energies $\Sigma^{r,a,K}(\omega)$ associated to the E_J term in the Hamiltonian, which would allow us to evaluate the needed GFs as

$$\begin{aligned} D^{r,a}(\omega) &= \left[\left(D_0^{r,a}(\omega)\right)^{-1} - \Sigma^{r,a}(\omega)\right]^{-1}, \\ D^K(\omega) &= [1+D^r(\omega)\Sigma^r(\omega)]D_0^K(\omega)\big[1+\Sigma^a(\omega)D_0^a(\omega)\big] \\ &\quad + D^r(\omega)\Sigma^K(\omega)D^a(\omega). \end{aligned} \tag{10}$$

To lowest order in E_J, we have [22]

$$\Sigma^{r,a(1)}(\omega) = E_J\exp\left[-\frac{i}{4}D_0^K(t=0)\right] \to 0\,, \tag{11}$$

since $\mathrm{Im}D_0^K(t=0) \to -\infty$ for $\omega_c \to 0$. One also obtains $\Sigma^{K(1)}(\omega) = 0$, as it corresponds to an effective static potential. To get the frequency-dependent corrections, it is then necessary to go to higher order. To second order in E_J, we find [22]

$$\begin{aligned} \Sigma^{r(2)}(t) &= E_J^2\sin\frac{D_0^r(t)}{2}\exp\left[\frac{i}{2}\left(D_0^K(t)-D_0^K(0)\right)\right] - B\delta(t), \\ \Sigma^{K(2)}(t) &= -iE_J^2\cos\frac{D_0^r(t)}{2}\cos\frac{D_0^a(t)}{2} \\ &\quad\times\ \exp\left[\frac{i}{2}\left(D_0^K(t)-D_0^K(0)\right)\right], \end{aligned} \tag{12}$$

where B is a constant such that $\Sigma^{r(2)}(\omega=0) = 0$.

From these expressions, one can obtain numerical results for the self-energies [23]. In addition, fully analytical results for the Keldysh self-energies can be obtained in the limit $(R_L+R_R)/R_Q \to 1$ and $T_j \to 0$ [23] (see also comments below). Let us also mention that this perturbative analysis leads

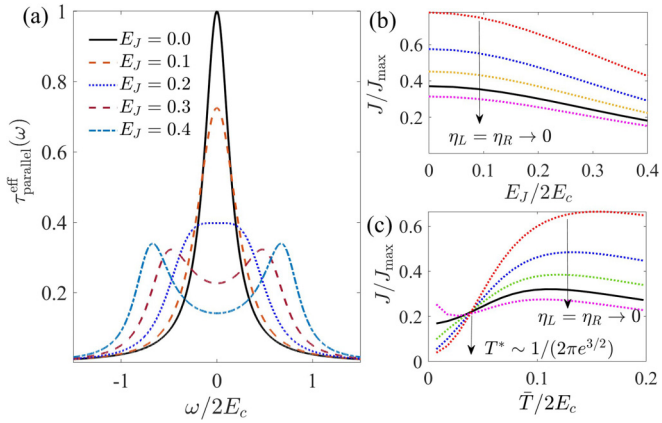

FIG. 2. (a) Effective heat transmission coefficient in the parallel configuration for increasing E_J values (from 0 to 0.4) and $T_L = 0.2, T_R = 0.1, \omega_c = 2 \times 10^{-3}$ (in units of $2E_c$) and $\eta_{L,R} = 1/4\pi$. (b) Total heat current J, normalized to the maximum heat current for a ballistic channel $J_{\rm max}$, as a function of E_J. The full line corresponds to the parameters in (a), while the dashed lines illustrate its behavior with $\eta_L = \eta_R$ varying between $1/\pi$ to $1/5\pi$. (c) $J/J_{\rm max}$ for $E_J = 0.2$ as a function of mean temperature $\bar{T} = (T_L + T_R)/2$ in the linear response regime for the same $\eta_L = \eta_R$ range.

to the same predictions as dynamical Coulomb blockade theory that were used in Ref. [16] for fitting the IV curves [23].

Replacing these results into Eq. (10), we obtain the results in Fig. 2(a) for the heat transmission coefficient, which exhibits a strong dependence on E_J, in spite of the full suppression of the dc Josephson effect that occurs in the insulating phase [24] for this parameter range. As shown in Fig. 2(b), the total heat current in this configuration decreases with increasing E_J, and, as illustrated by the dashed lines in this panel, the sensitivity of the total heat current with E_J exhibits a strong dependence on the lead resistances.

One gets more insight by analyzing the low frequency renormalization of the heat transmission coefficient $\tau_{\rm parallel}(\omega)$. In fact, at low frequencies $\Sigma^{r(2)}(\omega) \sim -i\delta\eta\omega + \delta m\omega^2$, where $\delta\eta$ and δm provide renormalization of the damping and mass model parameters. An analytical expression for the temperature and resistance scaling of these effective parameters is presented in Ref. [23]. At low temperatures ($T_{L,R} \ll \gamma$) and for $\eta_{L,R} \sim 1/2\pi$, we obtain

$$\delta\eta \sim \left(\frac{E_J}{\gamma}\right)^2 \left(\frac{\eta_L T_L + \eta_R T_R}{m^2\gamma^2}\right)^{-2} \prod_j \left(\frac{T_j}{\gamma}\right)^{\eta_j/\pi m^2\gamma^2}, \quad (13)$$

where $\gamma = (\eta_L + \eta_R)/m$. Note that for $T_L = T_R = T$ and $\alpha_L = \alpha_R = \alpha/2$, the SB transition at $\alpha = 1$ is encoded in the scaling law $\sim T^{2/\alpha-2}$, which results for the renormalization of the damping parameter [22,25].

In terms of these renormalized parameters, $\tau_{\rm parallel}(\omega)$ at low frequencies can be written as

$$\tau^{\rm eff}_{\rm parallel}(\omega) \simeq \frac{4\eta_L\eta_R}{\tilde{m}^2\omega^2 + \tilde{\eta}^2} \frac{\tilde{\eta}}{\eta_L + \eta_R}, \quad (14)$$

where $\tilde{\eta} = \eta_L + \eta_R + \delta\eta$ and $\tilde{m} = m - \delta m$. This expression accounts for the qualitative behavior of the heat transmission coefficient that can be observed in Fig. 2(a), i.e., a suppression and broadening of the $\omega \sim 0$ peak for increasing E_J. Note that the peaks observed in the transmission coefficient for higher frequencies and finite E_J (see Fig. 2) arise from the self-energy structure, which includes a mass renormalization that saturates for $\omega/2E_c \sim 1$.

On the other hand, lower temperatures are required to observe signatures of the SB transition in the heat transport properties. In Fig. 2(c), we show the heat current J as a function of $\bar{T} = (T_L + T_R)/2$ in the linear regime ($\delta T = T_L - T_R \to 0$) for different values of $\eta_L = \eta_R$, ranging from $1/\pi$ to $1/5\pi$, i.e., across the transition which for the parallel case should occur at $\eta_{L,R} = 1/4\pi$. While for $\bar{T} \gtrsim \gamma, J$ decreases with increasing resistance due to the narrowing of the $\tau^{\rm eff}_{\rm parallel}(\omega)$ zero-frequency peak, the tendency is reversed at low temperatures ($\bar{T} \ll \gamma$) due to the divergence of $\delta\eta$ for $\alpha > 1$. The transition between these two opposite behaviors occurs around $\bar{T} = T^* \sim 1/(2\pi e^{3/2})$, where the damping renormalization is weakly dependent on the environment resistance [23]. This behavior is similar to the nonmonotonous dependence of the mobility found for quantum Brownian motion in a periodic potential [26].

Series configuration. In the actual setup in Ref. [16], left and right leads are placed in a loop for the heat current measurements, which actually corresponds to a *series* connection, as depicted in Fig. 1(b). One should describe this situation in terms of two phase variables φ_1 and φ_2, each one coupled to the left and right reservoirs respectively, while the charge N through the junction is conjugate to $\varphi_1 - \varphi_2$. Consequently, Eq. (1) should be modified by replacing the Josephson term by $-E_J\cos(\varphi_1 - \varphi_2)$ and φ by φ_j in the coupling to the environmental modes. Thus, the bare GFs adopt a matrix form in the $\varphi_{1,2}$ space and can be obtained from the following equations:

$$\begin{pmatrix} m(\omega^2 - \omega_c^2) \pm i\omega\eta_L & -m(\omega^2 - \omega_c^2) \\ -m(\omega^2 - \omega_c^2) & m(\omega^2 - \omega_c^2) \pm i\omega\eta_R \end{pmatrix} \hat{D}_0^{r,a} = \hat{I}, \quad (15)$$

and $\hat{D}_0^K = \hat{D}_0^r \hat{d}_0^K \hat{D}_0^a$, where

$$\hat{d}_0^K = -2i\omega\,\mathrm{diag}[\eta_L \coth(\beta_L\omega/2); \eta_R \coth(\beta_R\omega/2)].$$

To include the effect of finite E_J in this configuration, the corresponding self-energies in Eq. (12) have to be expressed in terms of $\tilde{D}_0(t) = \mathrm{Tr}[\hat{D}_0(t)(\hat{I} - \sigma_x)]$, where σ_x is a Pauli matrix in $\varphi_{1,2}$ space. The resulting self-energies $\tilde{\Sigma}^{r,K}(\omega)$ exhibit a similar behavior as in the parallel configuration (see Supplemental Material (SM) [23]).

On the other hand, the Dyson equations for the dressed GFs (10) acquire a matrix form in the $\varphi_{1,2}$ space and the corresponding self-energies are obtained from $\tilde{\Sigma}^{r,a,K}$ as $\hat{\Sigma}^{r,a,K} = \tilde{\Sigma}^{r,a,K}(\hat{I} - \sigma_x)$.

The heat current in the series connection cannot be expressed in the compact form (6). It is, in contrast, necessary to reproduce the steps leading to Eq. (5) to derive the corresponding expression for the heat current in the series connection

$$J_j = \int d\omega\omega^2\eta_j \mathrm{Im}\left[D^r_{l_j l_j}(\omega)(1+2n_j(\omega)) - \frac{D^K_{l_j l_j}(\omega)}{2}\right], \quad (16)$$

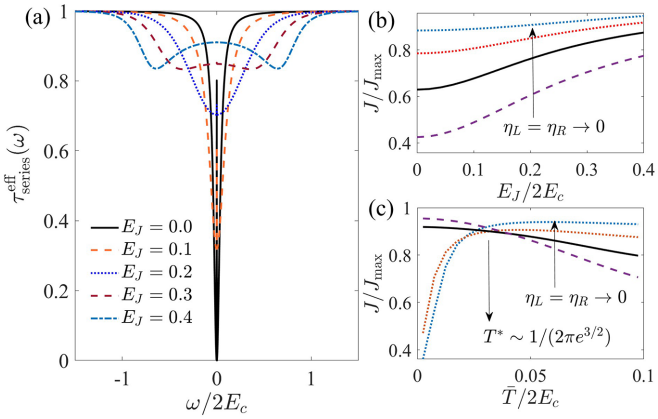

FIG. 3. Same as Fig. 2 but for the series configuration. The parameters in (a) are the same as those in Fig. 2(a) while in (b) and (c) the full lines correspond to $\eta_L = \eta_R = 1/\pi$, where the SB transition occurs for this configuration.

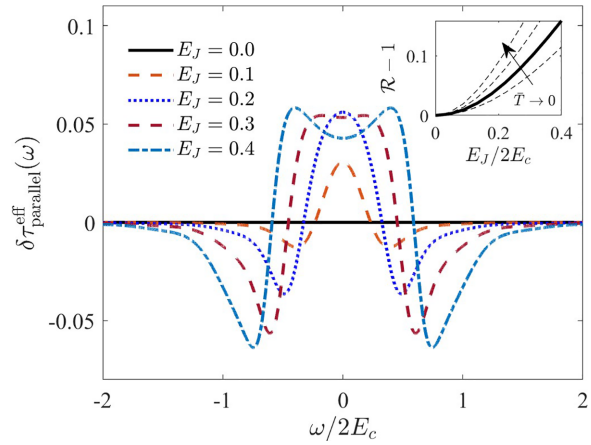

FIG. 4. Asymmetry in the heat transmission coefficient $\delta\tau^{\rm eff}(\omega) = \tau^{\rm eff(+)}_{\rm parallel}(\omega) - \tau^{\rm eff(-)}_{\rm parallel}(\omega)$ for the parallel configuration with $\eta_L = 1/\pi$, $\eta_R = 1/4\pi$, $\Delta T = 0.1$, $\bar{T} = (T_L + T_R)/2 = 0.15$, and increasing values of E_J from 0 to 0.4. The corresponding heat rectification ratio $\mathcal{R} = |J^+/J^-|$ as a function of E_J is shown as a full line in the inset. The dashed lines illustrate its variation with $\bar{T}$ from 0.175 to 0.1.

where $l_j = 1, 2$ for $j = L, R$ respectively. This expression can be decomposed [23] as $J_j = (-1)^{l_j} J^{\rm el} + J^{\rm in}_j$, where $J^{\rm el} = \int d\omega \hbar\omega \tau^{\rm eff}_{\rm series}(\omega)[n_L(\omega) - n_R(\omega)]$ corresponds to the *elastic* contribution with

$$\tau^{\rm eff}_{\rm series}(\omega) = 4\eta_L\eta_R\omega^2 \left|D^r_{12}(\omega)\right|^2 , \tag{17}$$

while the *inelastic* contribution is given by

$$J^{\rm in}_j = \int d\omega\omega^2\eta_j {\rm Im}[\hat{D}^r\{(\hat{\Sigma}^r - \hat{\Sigma}^a)(1+2n_j) - \hat{\Sigma}^K\}\hat{D}^a]_{l_j l_j} . \tag{18}$$

In the noninteracting case (i.e., $E_J = 0$), the inelastic term vanishes and the heat current can again be written in the usual Landauer form with a transmission coefficient at $\omega_c \to 0$,

$$\tau^0_{\rm series}(\omega) = \frac{4m^2\omega^2\eta_L\eta_R}{((\eta_L + \eta_R)m\omega)^2 + (\eta_L\eta_R)^2} , \tag{19}$$

which exhibits a zero frequency dip and tends to $4\eta_L\eta_R/(\eta_L + \eta_R)^2$ at large frequencies, as illustrated in Fig. 3.

The behavior of the effective transmission coefficient for finite E_J is illustrated in Fig. 3(a) for the same parameters as in Fig. 2(a). We observe that at finite E_J the zero frequency dip is progressively suppressed. On the other hand, the inelastic term provides an additional contribution to the heat current [23]. Thus, in contrast to the parallel configuration, there is a slight increase of the heat current with E_J, which is confirmed by the integrated results in Fig. 3(b). As can be observed, this increase is more pronounced as the leads resistances approach R_Q. This behavior is in qualitative agreement with the experimental results in Ref. [16]. On the other hand, the temperature dependence of $J/J_{\rm max}$ in the linear regime, illustrated in Fig. 3(c), exhibits a crossover at T^* as in the parallel case but with an opposite tendency with environmental resistance: it increases with increasing resistance (decreasing $\eta_{L,R}$) for $T > T^*$ and the opposite for $\bar{T} < T^*$. At the critical resistance ($\eta_L = \eta_R = 1/\pi$), the temperature variation of the heat conductance is minimal, which provides an alternative signature of the transition. Note that the experimental results of Ref. [16] exhibit a drop at the lower temperatures, consistent with an insulating behavior (see additional figure in the SM [23]).

Rectification properties. Another interesting property of a JJ in a resistive environment is its possible behavior as a heat rectifier. The JJ anharmonicity has been used to define thermal diodes based on weakly coupled qubits [27]; see also Ref. [18]. Though heat rectifiers using JJs have been measured in the absence of environmental effects (but additionally coupled to a phonon bath) [28] or in superconducting qubits [29,30] (see also Ref. [31] for a review), their rectifying properties in the insulating side of the SB transition have not been considered. For simplicity, we consider here only the parallel configuration with an asymmetry provided by $R_L \neq R_R$. We can then define a forward (J^+) and a reverse (J^-) heat current given by

$$J^{\pm} = \int \frac{d\omega}{\pi} \hbar\omega \tau^{\rm eff(\pm)}_{\rm parallel}(\omega)[n^{\pm}_L(\omega) - n^{\pm}_R(\omega)], \tag{20}$$

which correspond to positive and negative temperature bias $\Delta T = T_L - T_R$. As is customary, we also define a heat rectification ratio $\mathcal{R} = |J^+/J^-|$ which, as can be seen from Eq. (20), deviate from unity provided $\delta\tau^{\rm eff} \equiv \tau^{\rm eff(+)}_{\rm parallel} - \tau^{\rm eff(-)}_{\rm parallel} \neq 0$.

In Fig. 4, we show the behavior of $\delta\tau^{\rm eff}(\omega)$ for increasing values of E_J in an asymmetric configuration with $\alpha_L = 2$ and $\alpha_R = 0.5$. We observe that, for finite E_J, heat transport in the forward direction is favored at low frequencies, while the opposite occurs at higher frequencies. There is not, however, a compensation in the total heat current and thus one obtains that $\mathcal{R} > 1$, as illustrated in the inset of Fig. 4. Rectification ratios of the order of 10% or larger are obtained for the set of parameters in this figure. These ratios can increase further by decreasing the mean temperature $\bar{T} = (T_L + T_R)/2$ (see inset in Fig. 4).

Further insight on these properties can be obtained from the analytical approximation to the system self-energies. As

shown in Ref. [23], the rectification ratio in the parallel configuration can be expressed as

$$\mathcal{R} - 1 \sim (mE_J)^2 \frac{\eta_R - \eta_L}{\eta_L + \eta_R} \left(\frac{2}{\alpha} - 2 \right) \bar{T}^{\frac{2}{\alpha}-2} \frac{\delta T}{\bar{T}} \qquad (21)$$

in the limit $T_{L,R} \ll \gamma$ and $\alpha \gtrsim 1$ upon a small temperature difference $\delta T \ll \bar{T}$. This expression accounts for the main features of the numerical results, i.e., the quadratic increase with E_J and the increase of $\mathcal{R}$ as the mean temperature is decreased. Equation (21) also indicates that, as far as $\alpha > 1$, the heat current is larger when the colder reservoir corresponds to the one with larger resistance. This behavior is similar to the case of a two-level system with a nonseparable coupling to the heat baths [27,32]. Equation (21) also indicates that the SB transition could be detected by the change in sign of $\mathcal{R} - 1$ at $\alpha = 1$.

Conclusions. In summary, we have presented nonequilibrium Green's function calculations for photonic heat transport through a Josephson junction in a resistive environment. Our results are in qualitative agreement with the experimental ones from Ref. [16] and suggest how signatures of the SB transition can be detected in heat transport measurements at sufficiently low temperatures [33]. We further demonstrate rectification properties for this device that can be tested in future experiments.

Note added. Recently, we become aware of a related study [34] for the same system in the scaling regime, yielding results which are complementary to the ones in the present Letter.

Acknowledgments. The authors wish to thank M. Houzet and P. Joyez for enlightening discussions. A.L.Y. also acknowledges Professor U. Weiss for useful comments on the validity of the perturbative approach adopted in this Letter. We acknowledge funding from the Spanish Ministerio de Ciencia e Innovación via Grants No. PID2020-117671GB-I00, No. PID2019-110125GB-I00, and No. PID2022-142911NB-I00, and through the María de Maeztu Programme for Units of Excellence in R&D No. CEX2023-001316-M. This Letter was partially funded by the Research Council of Finland Centre of Excellence Program Grant No. 336810 and Grant No. 349601 (THEPOW).

[1] F. Tafuri, ed., *Fundamentals and Frontiers of the Josephson Effect* (Springer International Publishing, Cham, Switzerland, 2019).

[2] A. O. Caldeira and A. J. Leggett, Quantum tunnelling in a dissipative system, Ann. Phys. **149**, 374 (1983).

[3] J. Leppäkangas, G. Johansson, M. Marthaler, and M. Fogelström, Nonclassical photon pair production in a voltage-biased Josephson junction, Phys. Rev. Lett. **110**, 267004 (2013).

[4] S. Jebari, F. Blanchet, A. Grimm, D. Hazra, R. Albert, P. Joyez, D. Vion, D. Estève, F. Portier, and M. Hofheinz, Near-quantum-limited amplification from inelastic Cooper-pair tunnelling, Nature Electronics **1**, 223 (2018).

[5] A. Schmid, Diffusion and localization in a dissipative quantum system, Phys. Rev. Lett. **51**, 1506 (1983).

[6] S. A. Bulgadaev, Phase diagram of a dissipative quantum system, JETP Lett. **39**, 264 (1984).

[7] K. Masuki, H. Sudo, M. Oshikawa, and Y. Ashida, Absence versus presence of dissipative quantum phase transition in Josephson junctions, Phys. Rev. Lett. **129**, 087001 (2022).

[8] T. Sépulcre, S. Florens, and I. Snyman, Comment on "Absence versus presence of dissipative quantum phase transition in Josephson junctions," Phys. Rev. Lett. **131**, 199701 (2023).

[9] C. Altimiras, D. Esteve, Ç. Girit, H. le Sueur, and P. Joyez, Absence of a dissipative quantum phase transition in Josephson junctions: Theory, arXiv:2312.14754.

[10] O. Kashuba and R.-P. Riwar, Limitations of Caldeira-Leggett model for description of phase transitions in superconducting circuits, Phys. Rev. B **110**, 184505 (2024).

[11] L. Giacomelli and C. Ciuti, Emergent quantum phase transition of a Josephson junction coupled to a high-impedance multimode resonator, Nature Commun. **15**, 5455 (2024).

[12] A. Murani, N. Bourlet, H. le Sueur, F. Portier, C. Altimiras, D. Esteve, H. Grabert, J. Stockburger, J. Ankerhold, and P. Joyez, Absence of a dissipative quantum phase transition in Josephson junctions, Phys. Rev. X **10**, 021003 (2020).

[13] P. J. Hakonen and E. B. Sonin, Comment on "Absence of a dissipative quantum phase transition in Josephson junctions", Phys. Rev. X **11**, 018001 (2021); A. Murani, N. Bourlet, H. le Sueur, F. Portier, C. Altimiras, D. Esteve, H. Grabert, J. Stockburger, J. Ankerhold, and P. Joyez, Reply to "Comment on 'Absence of a dissipative quantum phase transition in Josephson junctions' ", *ibid.* **11**, 018002 (2021).

[14] R. Kuzmin, N. Mehta, N. Grabon, R. A. Mencia, A. Burshtein, M. Goldstein, and V. E. Manucharyan, Observation of the Schmid-Bulgadaev dissipative quantum phase transition, arXiv:2304.05806.

[15] J. P. Pekola and B. Karimi, *Colloquium:* Quantum heat transport in condensed matter systems, Rev. Mod. Phys. **93**, 041001 (2021).

[16] D. Subero, O. Maillet, D. S. Golubev, G. Thomas, J. T. Peltonen, B. Karimi, M. Marín-Suárez, A. L. Yeyati, R. Sánchez, S. Park, and J. P. Pekola, Bolometric detection of coherent Josephson coupling in a highly dissipative environment, Nat. Commun. **14**, 7924 (2023).

[17] G. Thomas, J. P. Pekola, and D. S. Golubev, Photonic heat transport across a Josephson junction, Phys. Rev. B **100**, 094508 (2019).

[18] T. Ojanen and A.-P. Jauho, Mesoscopic photon heat transistor, Phys. Rev. Lett. **100**, 155902 (2008).

[19] L. V. Keldysh, Diagram technique for nonequilibrium processes, Zh. Eksp. Teor. Fiz **47**, 1515 (1964) [Sov. Phys. JETP **20**, 1018 (1965)].

[20] Y. Meir and N. S. Wingreen, Landauer formula for the current through an interacting electron region, Phys. Rev. Lett. **68**, 2512 (1992).

[21] J. B. Pendry, Quantum limits to the flow of information and entropy, J. Phys. A: Math. Gen. **16**, 2161 (1983).

[22] U. Eckern and F. Pelzer, Quantum dynamics of a dissipative object in a periodic potential, Europhys. Lett. **3**, 131 (1987).

[23] See Supplemental Material at http://link.aps.org/supplemental/10.1103/PhysRevB.110.L220502 for details on the numerical calculations, analytical approximations and further insight on temperature dependence of the experimental results in Ref. [16].

[24] G.-L. Ingold and Y. V. Nazarov, Charge tunneling rates in ultrasmall junctions, in *Single Charge Tunneling*, edited by H. Grabert and M. Devoret (Springer, 1992), Chap. 2, p. 21.

[25] C. Aslangul, N. Pottier, and D. Saint-James, Quantum Brownian motion in a periodic potential: A pedestrian approach, J. Phys. France **48**, 1093 (1987).

[26] M. P. A. Fisher and W. Zwerger, Quantum Brownian motion in a periodic potential, Phys. Rev. B **32**, 6190 (1985).

[27] D. Segal and A. Nitzan, Spin-boson thermal rectifier, Phys. Rev. Lett. **94**, 034301 (2005).

[28] M. J. Martínez-Pérez and F. Giazotto, Efficient phase-tunable Josephson thermal rectifier, Appl. Phys. Lett. **102**, 182602 (2013).

[29] J. Senior, A. Gubaydullin, B. Karimi, J. T. Peltonen, J. Ankerhold, and J. P. Pekola, Heat rectification via a superconducting artificial atom, Commun. Phys. **3**, 40 (2020).

[30] R. Upadhyay, D. S. Golubev, Y.-C. Chang, G. Thomas, A. Guthrie, J. T. Peltonen, and J. P. Pekola, Microwave quantum diode, Nat. Commun. **15**, 630 (2024).

[31] L. Arrachea, Energy dynamics, heat production and heat–work conversion with qubits: Toward the development of quantum machines, Rep. Prog. Phys. **86**, 036501 (2023).

[32] Note that the temperature behaviour of the rectification is strongly system and parameter dependent.

[33] We notice that our calculations assume a purely Ohmic environment. Departures from this idealized case might lead to deviations from our predictions in an actual experiment [35].

[34] T. Yamamoto, L. I. Glazman, and M. Houzet, Thermal transport across a Josephson junction in a dissipative environment, Phys. Rev. B **110**, L060512 (2024).

[35] R. Daviet and N. Dupuis, Nature of the Schmid transition in a resistively shunted Josephson junction, Phys. Rev. B **108**, 184514 (2023).